THE JOURNAL OF BIOLOGICAL CHEMISTRY

Vol. 264, No. 32, Issue of November 15, pp. 18907-18911, 1989
Printed in U.S.A.

Determination of the Secondary Structure of Interleukin-8 by Nuclear Magnetic Resonance Spectroscopy*

(Received for publication, June 9, 1989)

G. Marius Clore‡§, Ettore Appella¶, Masaki Yamada‖, Kouji Matsushima, and Angela M. Gronenborn‡§**

*From the ‡Laboratory of Chemical Physics, National Institute of Diabetes and Digestive and Kidney Diseases, the ¶Laboratory of Cell Biology, National Cancer Institute, National Institutes of Health, Bethesda, Maryland 20892, ‖Research Laboratories, Dainippon Pharmaceutical Co., Ltd., Suita, Osaka 564, Japan, and the **Laboratory of Molecular Immunoregulation, Biological Response Modifiers Program, Division of Cancer Treatment, National Cancer Institute, Frederick, Maryland 21701*

The solution conformation of interleukin-8 (IL-8), a small protein of 72 residues with a wide range of proinflammatory activities, has been investigated by two-dimensional NMR spectroscopy. The ^{1}H-NMR spectrum of IL-8 is assigned in a sequential manner and regular elements of secondary structure are identified on the basis of a qualitative interpretation of the nuclear Overhauser, coupling constant and amide exchange data. The IL-8 monomer contains a triple stranded anti-parallel β-sheet arranged in a Greek key and a long C-terminal helix (residues 57–72). It is shown that IL-8 is a dimer in solution in which the interface is principally formed by six backbone hydrogen bonds between residues 25, 27, and 29 of one monomer and residues 29, 27, and 25, respectively, of the other. As a result, the two units of the dimer form a contiguous six-stranded anti-parallel β-sheet. The secondary structure of IL-8 is similar to that found in the crystal structure of the sequence related protein platelet factor 4.

Interleukin-8 (IL-8[1]; Ref. 1), also variously known as neutrophil activation factor (2) or peptide (3), monocyte derived chemotactic factor (4), mitogen-stimulated human leukocyte protein (5), and T cell chemotactic factor (1), is a small ~8 kDa basic protein which is released from several types of cells, including monocytes, fibroblasts, endothelial cells, and keratinocytes, by an inflammatory stimulus. *In vivo* and *in vitro* studies have shown that IL-8 possesses a wide range of proinflammatory activities which include neutrophil activation (6) and the selective capacity to attract neutrophils (4) and T cells (1). Sequence comparisons (4, 7) indicate that IL-8 bears sequence similarity to a family of molecules involved in inflammation and immune regulation comprising β-thromboglobulin, platelet factor 4 (PF4), γ-interferon-induced protein (γIP-10), and human growth related protein (Gro). β-Thromboglobulin and PF4 contain 4 cysteine residues at the same location of the amino acid chain which form two intrachain disulfide bridges (8). The location of the 4 cysteine residues in IL-8, γIP-10, and Gro is essentially identical to that in the other two proteins, suggesting that all four proteins may have similar polypeptide folds. A key to understanding the structure-function relationships of these proteins is a detailed knowledge of their three-dimensional structures. Up to now the only structural data available consists of the structure of PF4 (residues 24–85), recently solved by x-ray diffraction at a resolution of 3 Å (7). No structural information on any other member of the family has been obtained to our knowledge. An alternative to crystallography is the application nuclear magnetic resonance spectroscopy (NMR) which allows one to determine the three-dimensional structure of a protein in solution. In this paper we present the elucidation of the secondary structure of IL-8 based on ^{1}H NMR measurements as well as the complete assignment of the IL-8 spectrum.

EXPERIMENTAL PROCEDURES

Recombinant human IL-8 was expressed in *Escherichia coli* and purified as described in Ref. 9. Samples for NMR contained ~1.8 mM protein in either 99.996% D_2O or 90% H_2O/10% D_2O at pH 4.4 or 5.2. The following spectra were recorded at 600 MHz on a Bruker AM 600 spectrometer in both H_2O and D_2O: P.COSY (10), PE.COSY (11), with a 35 ° mixing pulse; NOESY (12), with mixing times of 50, 100, and 150 ms; and HOHAHA (13), with mixing times ranging from 30 to 55 ms. All spectra were recorded in the pure phase absorption mode using the time-proportional incrementation method (12). HOHAHA spectra were recorded using a WALTZ17 mixing pulse sandwiched between 1.5-ms trim pulses (13). In the case of NOESY and HOHAHA spectra recorded in H_2O, the water resonance was suppressed using a semi-selective jump-return read sequence (14, 15).

RESULTS AND DISCUSSION

Sequential resonance assignment was carried out using well established procedures (16, 17). In particular, spin systems were identified using HOHAHA, P.COSY, and PE.COSY spectra, while the NOESY spectra were used to demonstrate through-space connectivities. To resolve ambiguities arising from chemical shift degeneracy, spectra were recorded at two pH values (5.5 and 4.4) and two temperatures (40 and 25 °C). Examples of HOHAHA and NOESY spectra are shown in Fig. 1. A summary of the sequential connectivities is given in Fig. 2, and the complete list of assignments in Table I.

The secondary structure can be deduced from a qualitative interpretation of the short range NOE, $^3J_{HN\alpha}$ coupling con-

* This work was supported in part by the Intramural AIDS targeted Anti-viral Program of the Office of the Director of the National Institutes of Health (G. M. C. and A. M. G.). The costs of publication of this article were defrayed in part by the payment of page charges. This article must therefore be hereby marked "*advertisement*" in accordance with 18 U.S.C. Section 1734 solely to indicate this fact.

§ To whom correspondence should be addressed.

[1] The abbreviations used are: IL-8, interleukin-8; PF4, platelet factor 4; NOE, nuclear Overhauser effect; NOESY, two-dimensional nuclear Overhauser enhancement spectroscopy; P.COSY, two-dimensional primitive correlated spectroscopy; PE.COSY, two-dimensional primitive exclusive correlated spectroscopy; HOHAHA, two-dimensional homonuclear Hartmann-Hahn spectroscopy.

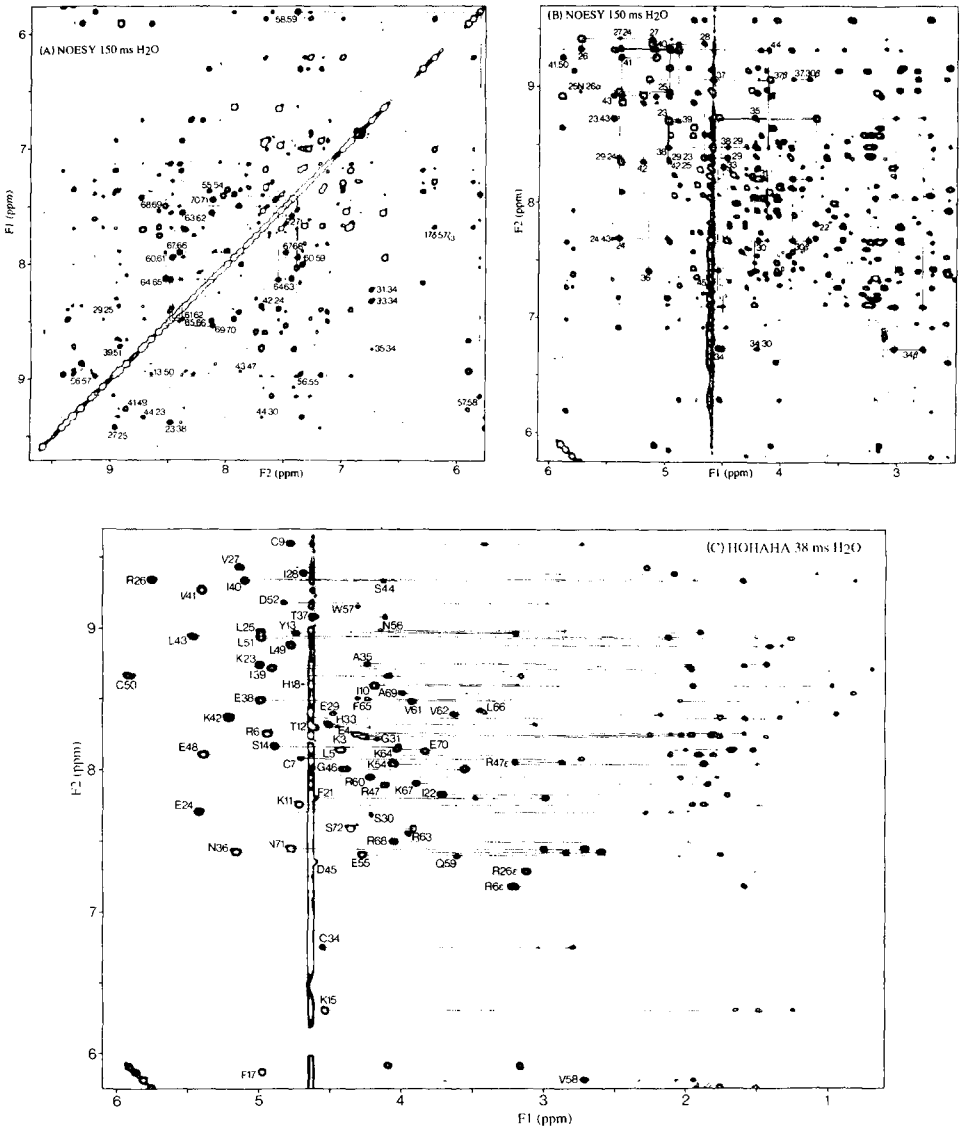

FIG. 1. **NOESY and HOHAHA spectra of IL-8 in 90% H_2O at pH 5.5 and 40 °C.** *A*, NH(F2)-NH(F1); and *B*, NH(F2)-C$^{\alpha}$H/C$^{\beta}$H(F1) regions of the 150-ms NOESY spectrum; *C*, NH(F2)-aliphatic(F1) region of the 38-ms HOHAHA spectrum. A stretch of sequential NH(i)-NH(i+1) NOE connectivities for the C-terminal helix together with a number of long range NH(i)-NH(j) NOEs are shown in *A*. A stretch of sequential C$^{\alpha}$H(i)-NH(i+1) NOE connectivities are shown in *B* with the labels at the intraresidue C$^{\alpha}$H(i)-NH(i) NOE cross-peaks. Also indicated in *B* are some C$^{\beta}$H(i)-NH(i+1) (denoted by the letter β) and long range C$^{\alpha}$H(i)-NH(j) connectivities. Direct and relayed through-bond connectivities involving the NH protons are shown in *C* with the labels at the direct NH-C$^{\alpha}$H connectivities.

stant and amide exchange data presented in Fig. 2, together with longer range NOEs involving backbone C$^{\alpha}$H and NH protons (16). No sequential NOEs could be observed for the three N-terminal residues suggesting that they are highly mobile and disordered in solution. The main body of the protein is formed by β-strands with long stretches of strong C$^{\alpha}$H(i)-NH(i+1) NOEs and a few turns and loops. The turns are centered around residues 9/10, 20/21, 45/46, 52/53, and 55/56. At the C terminus there is a long α-helix extending from residues 57 to 72, characterized by a stretch of NH(i)-NH(i+1,2), C$^{\alpha}$H(i)-NH(i+3,4) and C$^{\alpha}$H(i)-C$^{\beta}$H(i+3) NOEs, and small values of the $^3J_{HN\alpha}$ coupling constants. A schematic representation of the regular secondary structure elements is illustrated at the bottom of Fig. 2. The protein contains a triple-stranded anti-parallel β-sheet arranged in a Greek key (Fig. 3) with strand 2 (residues 36–43) hydrogen-bonded to strands 1 (residues 23–30) and 3 (residues 47–51). Strands 1 and 2 are connected by a loop (residues 31–35), and strands 2 and 3 by a 3:5 β-hairpin (residues 44–47) comprising a β-turn and G1 β-bulge (18). At the beginning of strand 1 there is a β-bulge at Lys-23, as evidenced by NOEs from Lys-23(NH) to Glu-24(NH), Leu-43(C$^{\alpha}$H), and Ser-44(NH), and from Glu-24(NH) to Lys-42(NH) and Leu43(C$^{\alpha}$H). As a result the NH protons of both Lys-23 and Glu-24 are hydrogen-bonded to the carbonyl oxygen atom of Lys-42.

The peptide bond for the 4 proline residues, Pro-16, -19, -32, and -53 is in the trans conformation as evidenced by the presence of strong C$^{\alpha}$H(i−1)-C$^{\delta}$H(Pro−i) sequential NOEs.

Analyzing the short range sequential NOEs, we noted seven short range NOEs and three slowly exchanging backbone NH protons (Leu-25, Val-27, and Glu-29) that at first sight appeared inconsistent with the notion of a β-strand structure

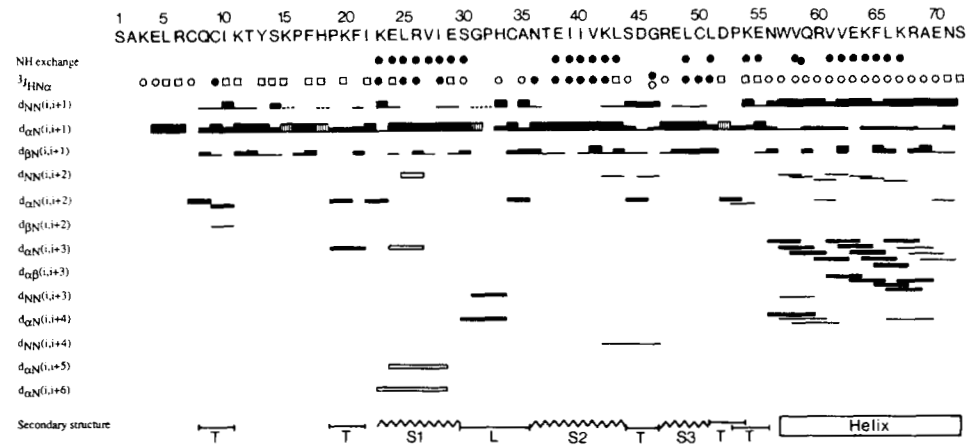

FIG. 2. **Summary of the sequential connectivities involving the NH, $C^{\alpha}H$, and $C^{\beta}H$ protons, as well as the $C^{\delta}H$ protons of proline, together with the $^3J_{HN\alpha}$ and amide exchange data.** The regular secondary structure elements deduced from the NMR data are also shown. The intensity of the NOEs are indicated by the *thickness of the lines.* Sequential connectivities involving the $C^{\delta}H$ protons of proline are indicated by a *dashed line* or a *box with vertical bars* along the same line as the corresponding connectivities involving NH protons. The four NOEs represented by *open boxes* arise from contacts at the dimer interface. Slowly exchanging amide protons that are still present in a HOHAHA spectrum recorded 12 h after dissolving the protein in D_2O are indicated by *closed circles* (●). The symbols for the $^3J_{HN\alpha}$ coupling constants are as follows: $J \leq 7$ Hz (○); 7 Hz $< J <$ 9 Hz, (□); $J \geq$ 9 Hz (●). The symbols for the secondary structure are as follows: *S*, strand; *T*; turn; *L*, loop.

for strand 1, in which residue 24, 26, and 28 from strand 1 are hydrogen bonded to residues 42, 40, and 38 of strand 2. The seven NOEs were as follows: $C^{\alpha}H(23)$-NH(29), $C^{\alpha}H(24)$-NH(27), $C^{\alpha}H(24)$-NH(29), $C^{\alpha}H(24)$-$C^{\alpha}H(28)$, NH(25)-NH(27), NH(25)-$C^{\alpha}H(26)$, and NH(25)-NH(29). These observations, however, are easily explained if IL-8 is a dimer, in which strand 1 from one molecule in the dimer forms an anti-parallel β-sheet comprising six hydrogen bonds with strand 1 of the other molecule (Fig. 3). In this manner, the two units of the dimer form a contiguous six-stranded anti-parallel β-sheet. This arrangement of the dimeric unit is identical to the one observed in the crystal structure of PF4 (7).

Confirmation that IL-8 is a dimer in solution was obtained by measuring the cross-relaxation rates for fixed distance interproton vectors in the aromatic rings of Phe-21, Trp-57, and Phe-65 using one-dimensional NOE measurements ($r_{C\delta\text{-}C\epsilon}$(Phe) = $r_{C\gamma\text{-}C\zeta 3}$(Trp) = $r_{C\epsilon 3\text{-}C\zeta 3}$(Trp) = 2.46 Å). The value of the measured cross-relaxation rates was 1.73 ± 0.23 s^{-1} at 25 °C. This corresponds to a correlation time of 6.7 ± 0.9 ns which is within the range (6–9 ns) predicted for the rotational diffusion time of a protein of ~16 kDa on the basis of the Stokes-Einstein equation (19). There is no indication of further oligomerization of IL-8 under the conditions employed. This is in contrast to results reported for PF4 which exists as a tetramer in solution (20). The crystal structure is also that of a tetramer (7) which can be divided into two nominal dimers, each dimer being maintained by six hydrogen bonds and a cluster of hydrophobic interactions.

The structural homology between IL-8 and PF4 is consistent with the observed 30% amino acid sequence homology for residues 6–68 of IL-8 and residues 24–85 of PF4. Indeed, the match of the hydrogen bonding patterns in the anti-parallel β-sheets between the two structures is almost perfect, including the hydrogen bonding at the dimer interface. There is one small difference, namely the presence of a hydrogen bond between the NH of Ser-30 and the carbonyl backbone oxygen atom of Asn-36 in IL-8, which is absent for the corresponding residues, Ala-47 and Ser-53, respectively, in PF4. The other difference between the two protein structures is in the length of the C-terminal helix. The helix starts at the same relative position, Trp-57 in IL-8 and Leu-74 in PF4. In the case of IL-8, the helix extends right up to the C terminus at residue Ser-72, while in the case of PF4 it stops four residues earlier at Gly-85 and the last two residues of PF4 are not visible in the electron density map. This minor difference may be due to the helix breaking properties of the glycine residue.

Further examination of the sequences of the two proteins indicates that in order to align the 4 cysteine residues (at positions 7, 9, 34, and 50 in IL-8, and at positions 25, 27, 51, and 67 in PF4), the triple stranded anti-parallel β-sheet and the C-terminal helix, the segment from residues 12–22 in IL-8 must contain an insertion relative to the corresponding segment from residues 28 to 39 in PF4. The NOEs from Thr-12($C^{\beta}H$) to Leu-51($C^{\alpha}H$) and Asp-52(NH) and from Tyr-13(NH) to Cys-50(NH) suggest the presence of a hydrogen bond between the NH of Tyr-13 and the CO of Cys-50, which corresponds to the Thr-31(NH)-Cys-67(CO) hydrogen bond in PF4. Thus, the insertion must lie beyond residue 13. In PF4, there are also two hydrogen bonds between Lys-61(NH) and His-38(CO) and between His-38(NH) and Asn-35(CO). The Lys-61(NH)-His-38(CO) hydrogen bond in PF4 corresponds to a hydrogen bond between the NH of Ser-44 and the CO of Phe-21, as evidenced by NOEs from Ser-44(NH) to Phe-21($C^{\alpha}H$), Ile-22($C^{\alpha}H$) and Lys-23(NH). There is no evidence, however, that the NH of Phe-21, unlike that of His-38 in PF4, is involved in a hydrogen bonding interaction. The presence of NOEs from Pro-19($C^{\alpha}H$) to Phe-21(NH) and Ile-22(NH) suggests that residues 19–22 form a turn with a potential hydrogen bond between Pro-19(CO) and Ile-22(NH). Thus, the sequence Pro-36 to Ile-39 in PF4 corresponds to Pro-19 to Ile-22 in IL-8, with an insertion at position 18.

A more detailed comparison of the structures of IL-8 and PF4 will have to await the determination of the three-dimensional structure of IL-8 in solution which is currently in progress in our laboratory.

TABLE I

Proton resonance assignments of IL-8 at 40°C at pH 5.2

Chemical shifts are expressed relative to 4,4-dimethyl-4-silapentane 1-sulfonate.

Residue	NH	$C^{\alpha}H$	$C^{\beta}H$	Others
S1		4.16	4.01	
A2	8.22	4.39	1.43	
K3	8.22	4.25	1.77	
E4	8.24	4.30	2.02, 1.95	$C^{\gamma}H$ 2.25, 2.25
L5	8.13	4.42	1.69, 1.54	$C^{\gamma}H$ 1.61; $C^{\delta}H_3$ 0.90, 0.82
R6	8.24	4.92	2.10, 1.80	$C^{\gamma}H$ 1.58; $C^{\delta}H$ 3.20; $N^{\epsilon}H$ 7.18
C7	8.07	4.69	4.04, 2.72	
Q8	11.94	4.24	2.14, 2.03	$C^{\gamma}H$ 2.41, 2.30; $N^{\epsilon}H_2$ 7.55, 6.63
C9	9.58	4.76	3.40, 2.72	
I10	8.58	4.18	1.94	$C^{\gamma}H_3$ 0.96; $C^{\gamma}H_2$ 1.49, 1.25; $C^{\delta}H_3$ 0.89
K11	7.75	4.69	1.94, 1.87	$C^{\gamma}H$ 1.49, 1.44; $C^{\delta}H$ 1.77; $C^{\epsilon}H$ 3.06
T12	8.29	4.59	4.21	$C^{\gamma}H_3$ 1.04
Y13	8.95	4.73	3.18, 3.18	$C^{\delta}H$ 7.36; $C^{\epsilon}H$ 7.19
S14	8.15	4.87	4.02, 3.99	
K15	6.29	4.57	1.64, 1.47	$C^{\gamma}H$ 1.23; $C^{\delta}H$ 1.66; $C^{\epsilon}H$ 2.96
P16		1.63	1.21, 1.07	$C^{\gamma}H$ 1.45, 0.17; $C^{\delta}H$ 3.50, 3.17
F17	5.86	4.96	3.23, 3.16	$C^{\delta}H$ 7.68; $C^{\epsilon}H$ 7.34; $C^{\zeta}H$ 7.17
H18	8.59	4.67	3.29, 3.17	$C^{\epsilon 1}H$ 7.83; $C^{\delta 2}H$ 7.23
P19		4.44	2.56, 2.13	$C^{\gamma}H$ 1.98, 1.93; $C^{\delta}H$ 3.98, 2.82
K20	11.53	4.30	1.83, 1.74	$C^{\gamma}H$ 0.32; $C^{\delta}H$ 1.10, 0.91; $C^{\epsilon}H$ 2.35
F21	7.79	4.59	3.44, 2.98	$C^{\delta}H$ 7.70; $C^{\epsilon}H$ 7.53; $C^{\zeta}H$ 7.39
I22	7.82	3.70	1.69	$C^{\gamma}H_3$-0.07; $C^{\gamma}H_2$ 0.91, 0.79; $C^{\delta}H_3$ 0.31
K23	8.72	4.98	2.00, 1.59	
E24	7.69	5.40	2.08, 1.98	$C^{\gamma}H$ 2.26, 2.26
L25	8.96	4.97	1.90, 1.35	$C^{\gamma}H$ 1.50; $C^{\delta}H_3$ 0.99, 0.85
R26	9.33	5.74	1.74, 1.51	$C^{\gamma}H$ 1.89, 1.80; $C^{\delta}H$ 3.11; $N^{\epsilon}H$ 7.28
V27	9.42	5.12	2.26	$C^{\gamma}H_3$ 1.10, 0.80
I28	9.38	4.67	2.07	$C^{\gamma}H_3$ 1.08; $C^{\gamma}H_2$ 1.43, 0.99; $C^{\delta}H_3$ 0.87
E29	8.39	4.47	2.46, 2.24	$C^{\gamma}H$ 3.14, 3.14
S30	7.67	4.20	3.91, 3.76	
G31	8.21	4.23, 4.14		
P32		4.21	2.37, 1.79	$C^{\gamma}H$ 2.04, 1.99; $C^{\delta}H$ 3.84, 3.66
H33	8.31	4.50	3.05, 3.05	$C^{\epsilon 1}H$ 8.02; $C^{\delta 2}H$ 7.10
C34	6.74	4.54	3.02, 2.78	
A35	8.73	4.23	1.42	
N36	7.41	5.14	2.83, 2.58	$N^{\delta}H_2$ 7.53, 6.96
T37	9.07	4.59	4.10	$C^{\gamma}H_3$ 0.96
E38	8.48	4.98	2.03, 2.03	$C^{\gamma}H$ 2.48, 2.48
I39	8.71	4.90	1.95	$C^{\gamma}H_3$ 0.70; $C^{\gamma}H_2$ 1.53, 1.12; $C^{\delta}H_3$ 0.69
I40	9.32	5.09	1.59	$C^{\gamma}H_3$ 0.80; $C^{\gamma}H_2$ 1.47, 1.15; $C^{\delta}H_3$ 0.75
V41	9.26	5.39	2.07	$C^{\gamma}H_3$ 0.95, 0.88
K42	8.37	5.20	1.75, 1.58	$C^{\gamma}H$ 1.33; $C^{\delta}H$ 1.59; $C^{\epsilon}H$ 2.88
L43	8.93	5.45	2.13, 1.50	$C^{\gamma}H$ 1.32; $C^{\delta}H_3$ 0.33, 0.29
S44	9.32	4.11	4.19, 3.93	
D45	7.33	4.61	3.04, 2.50	
G46	7.99	4.18, 3.55		
R47	7.88	4.10	1.83, 1.31	$C^{\gamma}H$ 1.57; $C^{\delta}H$ 3.19, 2.86; $N^{\epsilon}H$ 8.04
E48	8.09	5.38	1.90, 1.80	$C^{\gamma}H$ 2.10, 2.10
L49	8.86	4.76	1.40, 1.31	$C^{\gamma}H$ 1.13; $C^{\delta}H_3$ 0.50, 0.10
C50	8.65	5.90	4.07, 3.15	
L51	8.29	4.97	1.50, 1.27	$C^{\gamma}H$ 1.02; $C^{\delta}H_3$ 0.80
D52	9.17	4.81	2.97, 2.56	
P53		4.02	3.40, 3.25	$C^{\gamma}H$ 1.97, 1.84; $C^{\delta}H$ 4.22, 4.15
K54	8.03	4.03	1.85, 1.85	$C^{\gamma}H$ 1.48; $C^{\delta}H$ 1.74; $C^{\epsilon}H$ 3.06
E55	7.39	4.26	1.83, 1.64	$C^{\gamma}H$ 2.39, 2.22
N56	8.96	4.12	2.99, 2.84	$N^{\delta}H_2$ 7.67, 6.94
W57	9.14	4.29	3.51, 3.27	$C^{\delta}1H$ 7.61; $C^{\zeta 2}H$ 7.28; $C^{\eta}H$ 7.00; $C^{\zeta 3}H$ 6.21; $C^{\epsilon 3}H$ 7.30; $N^{\epsilon 1}H$ 10.12
V58	5.80	2.70	1.93	$C^{\gamma}H_3$ 0.33, −0.42
Q59	7.38	3.60	4.04, 2.05	$C^{\gamma}H$ 2.57, 1.93; $N^{\epsilon}H_2$ 7.93, 6.62
R60	7.93	4.21	2.04, 1.92	$C^{\gamma}H$ 1.79, 1.79; $C^{\delta}H$ 3.26, 3.26
V61	8.47	3.91	2.28	$C^{\gamma}H_3$ 1.21, 1.13
V62	8.38	3.62	2.17	$C^{\gamma}H_3$ 0.93, 0.93
E63	7.54	3.93	2.24, 2.16	$C^{\gamma}H$ 2.40, 2.40
K64	8.13	4.02	2.00, 1.85	$C^{\gamma}H$ 2.06, 1.59; $C^{\delta}H$ 1.69; $C^{\epsilon}H$ 3.00
F65	8.50	4.23	3.27, 3.21	$C^{\delta}H$ 7.14; $C^{\epsilon}H$ 7.20; $C^{\zeta}H$ 6.93
L66	8.41	3.43	1.68, 1.60	$C^{\gamma}H$ 1.68; $C^{\delta}H_3$ 0.86, 0.86
K67	7.89	3.89	1.85, 1.80	$C^{\gamma}H$ 1.53, 1.49; $C^{\delta}H$ 1.64; $C^{\epsilon}H$ 2.95
R68	7.49	4.04	1.96, 1.83	$C^{\gamma}H$ 1.69, 1.41; $C^{\delta}H$ 3.00
A69	8.53	3.98	0.81	
E70	8.12	3.82	2.10, 2.04	$C^{\gamma}H$ 2.57, 2.57
N71	7.43	4.75	2.99, 2.65	$N^{\delta}H_2$ 7.66, 6.94
S72	7.67	4.14	3.90	

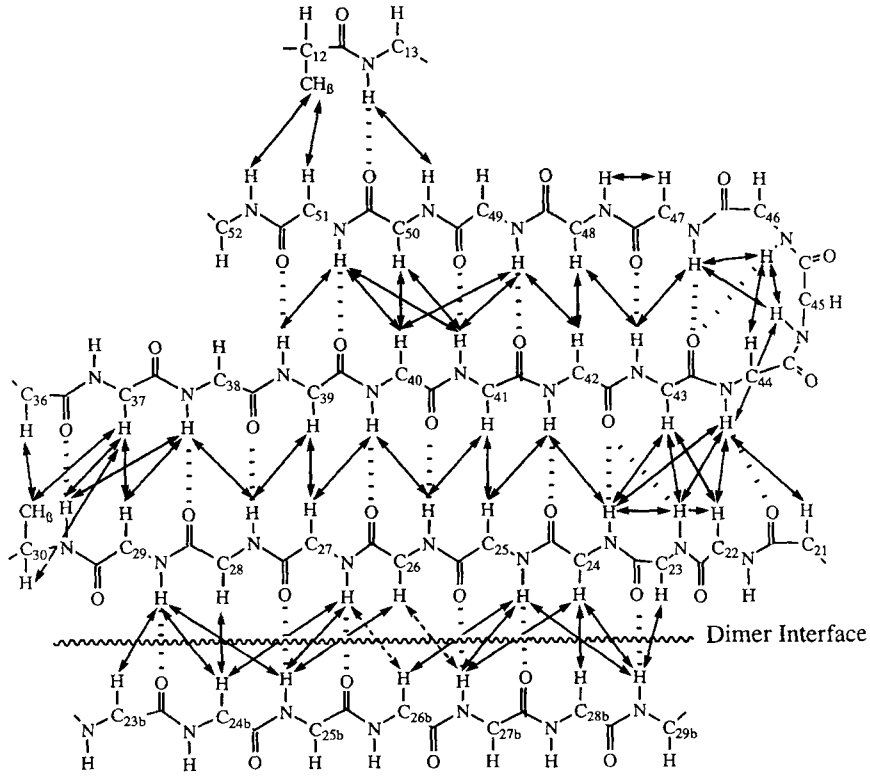

FIG. 3. **Schematic representation of the anti-parallel β-sheet structure and dimer interface of IL-8 deduced from a qualitative analysis of the NMR data.** The observed interstrand NOE connectivities between backbone NH and $C^{\alpha}H$ or $C^{\beta}H$ protons are indicated by *arrows*, and hydrogen bonds deduced from the NOE patterns and slowly exchanging amide protons are shown as *dashed lines*. (The NOE between Arg-26($C^{\alpha}H$) and Val-27(NH) arises both from a sequential connectivity along the strand, as well as from close proximity across the dimer interface; this particular NOE is therefore indicated by a *dashed line connecting the arrows*.)

REFERENCES

1. Larsen, C. G., Anderson, A. O., Appella, E., Oppenheim, J. J., and Matsushima, K. (1989) *Science* **243,** 1464–1466
2. Walz, A., Peveri, P., Aschauer, H., and Baggiolini, M. (1987) *Biochem. Biophys. Res. Commun.* **149,** 755–761
3. Gregory, H., Young, J., Schröder, J.-M., Mrowietz, U., and Christophers, E. (1988) *Biochem. Biophys. Res. Commun.* **151,** 883–980
4. Yoshimura, T., Matsushima, K., Tanaka, S., Robinson, E. A., Appella, E., Oppenheim, J. J., and Leonard, E. (1987) *Proc. Natl. Acad. Sci. U. S. A.* **84,** 9233–9237
5. Schmid, J., and Weissmann, C. (1987) *J. Immunol.* **139,** 250–256
6. Thelen, M., Peveri, P., Kernen, P., von Tscharner, V., Walz, A., and Baggiolini, M. (1988) *FASEB J.* **2,** 2702–2706
7. St. Charles, R., Walz, D. A., and Edwards, B. F. P. (1989) *J. Biol. Chem.* **264,** 2092–2099
8. Begg, G. S., Pepper, D. S., Chesterman, C. N., and Morgan, F. J. (1978) *Biochemistry* **17,** 1739–1744
9. Furuta, R., Yamagishi, J., Kotani, H., Sakamoto, F., Fukui, T., Matsui, Y., Sohmura, Y., Yamada, M., Yoshimura, T., Larsen, C. G., Oppenheim, J. J., and Matsushima, K. (1989) *J. Biochem. (Tokyo)* **106,** 436–441
10. Marion, D., and Bax, A. (1988) *J. Magn. Reson.* **80,** 528–533
11. Mueller, L. (1987) *J. Magn. Reson.* **72,** 191–196
12. Ernst, R. R., Bodenhausen G., and Wokaun, A. (1986) *Principles of Nuclear Magnetic Resonance in One and Two Dimensions,* Clarendon Press, Oxford
13. Bax, A. (1989) *Methods Enzymol.* **176,** 151–158
14. Plateau, P., and Gueron, M. (1982) *J. Am. Chem. Soc.* **104,** 7310–7311
15. Bax, A., Sklenar, V., Clore, G. M., and Gronenborn, A. M. (1987) *J. Am. Chem. Soc.* **109,** 6511–6513
16. Wüthrich, K. (1986) *NMR of Proteins and Nucleic Acids,* John Wiley & Sons, New York
17. Clore, G. M., and Gronenborn, A. M. (1987) *Protein Eng.* **1,** 275–288
18. Sibanda, B. L., and Thornton, J. M. (1985) *Nature* **316,** 170–174
19. Cantor, C. R., and Schimmel, P. R. (1980) *Biophysical Chemistry,* Part II, W. H. Freeman & Co., San Francisco
20. Bock, P. E., Luscombe, M., Marshall, S. E., Pepper, D. S., and Holbrook, J. J. (1980) *Biochem. J.* **191,** 769–776